On the droplet size and application of wettability analysis for the development of ink and printing substrates

Gruber, M., Waugh, D., Lawrence, J., Langer, N. & Scholz, D.

Original citation & hyperlink:
Gruber, M, Waugh, D, Lawrence, J, Langer, N & Scholz, D 2019, 'On the droplet size and application of wettability analysis for the development of ink and printing substrates', Langmuir, vol. 35, no. 38, pp. 12356-12365.
https://dx.doi.org/10.1021/acs.langmuir.9b01674

DOI 10.1021/acs.langmuir.9b01674
ISSN 0743-7463
ESSN 1520-5827

Publisher: American Chemical Society

On the droplet size and application of wettability analysis for the development of ink and printing substrates

M. GRÜßER[1], D.G. WAUGH*[2], J. LAWRENCE[2], N. LANGER[1] AND D. SCHOLZ[1]

[1]DataPhysics Instruments GmbH, Raiffeisenstraße 34, 70794 Filderstadt, Germany
[2]School of Mechanical, Aerospace and Automotive Engineering, Faculty of Engineering, Environment and Computing, Coventry University, Gulson Road, Coventry, CV1 2JH, UK

*Corresponding Author: david.waugh@coventry.ac.uk

Abstract:

For the printing industry to grow and for companies in the field to remain competitive, there is a drive towards enhancing research and development so that costs of inks and substrates can be minimised. This paper details one of the first studies into the importance of liquid droplet size for applying wettability science to the development of inks and substrates, using a newly developed picolitre droplet dispensing system (PDDS). Differences between using microlitre, µl (0.2 µl to 5µl), and picolitre, pl (15 pl to 380 pl), droplets for wettability analysis is considered, showing the importance of using pl droplets within the development of inks and substrates for printing applications. This is owed to differences in contact angle being up to 40° when comparing results from pl- and µl-sized water-based droplets. Wetting, absorption and evaporation behaviour of different droplet sizes are also discussed with specific consideration to the use of wettability science for ink development and the development of inkjet printing substrates. A newly developed commercially available water-based blue ink and a commercially available water-based black ink are studied using pl experimentation to show how pl-sized droplets for inkjet wettability analysis is the optimum volume range to ensure optimised inkjet printing analysis and development.

Keywords: Wettability; contact angle; wetting; ink; paper; picolitre droplets.

Introduction

Within the UK it is believed that the £3.7 billion paint, coatings and printing ink manufacturing industry is expected to contract and has been the case for the last five years (annual growth of -1.4% by the end of 2019) [1]. Having said that, the industrial ink printing market, globally was estimated at 4 million metric ton, by volume, in 2017 and is likely to reach a size of £16.3 billion in revenue terms by 2023 [2]. Because of these factors, there is a requirement to minimize the development costs associated with inks and substrates for inkjet printing. The scientific community is now moving towards the application of wettability science to measure the wetting behaviour associated with inks and to characterize substrate and ink interface properties [3-8]. This includes the determination of contact angles, surface energies/surface tensions, prediction of wetting behaviour and the study and the determination of absorption/evaporation behaviours. Wettability science technologies can also now be used to emulate the final printing process during the early stages of development. This will also likely enhance the optimization process for the compatibility determination of inks and substrates.

If one was to consider a static droplet of liquid on a solid surface, the contact angle, θ, as depicted in Figure 1, is given by the Young Equation (Equation (1)) [9,10], describing the equilibrium forces at the 3-phase contact line. The Young Equation (Equation (1)) provides the relationship between the surface tension of the liquid, σ_l, the surface energy of the solid surface, σ_s, and the solid-liquid interfacial energy γ_{sl}; where γ_{sl} is dependent on the adhesive bonds between that of the solid and that of the liquid.

$$\sigma_s = \gamma_{sl} + \sigma_l \cdot \cos\theta \quad (1)$$

Figure 2 shows a schematic diagram of the wetting nature at various values of contact angle on a solid surface. When a water contact angle, $\theta_w = 0°$, the solid's surface free energy tends to be very high and there is complete wetting of the substrate, with the liquid spreading across the surface. For $\theta_w < 90°$, the solid surface is generally termed as hydrophilic [11] and tends to have a good wetting nature. For $\theta_w > 90°$, this is generally termed hydrophobic [11] and tends to have a bad wetting nature. When $\theta_w > 150°$, the solid surface is known to be superhydrophobic [12-16] and there is no wetting of the solid surface. This is known as two separate phenomena: the lotus leaf effect [12,17] and the rose petal effect [18-21].

Fowkes [22] is known as a pioneer of approaching the analysis of wettability characteristics by partitioning the surface free energy into individual components, as shown in Equation (2). This approach was modified by Owens, Wendt, Rabel and Kaelble (OWRK) [23,24] by assuming that all of the components on the right hand side of Equation (2), apart from γ_s^d, can be associated with and incorporated into a polar component, γ_s^p, of the total surface free energy, γ^T . This approach is commonly known as the OWRK Method and enables the determination of γ^T [25-27].

$$\gamma^T = \gamma_s{}^d + \gamma_s{}^p + \gamma_s{}^h + \gamma_s{}^i + \gamma_s{}^{ab} + \gamma_s{}^o \quad (2)$$

$$\gamma^T = \gamma_s + \gamma_l - 2\left(\gamma_s{}^d \gamma_l{}^d\right)^{0.5} - 2\left(\gamma_s{}^p \gamma_l{}^p\right)^{0.5} \quad (3)$$

where γ_s^d, γ_s^p, γ_s^h, γ_s^i and γ_s^{ab} are the dispersive, polar, hydrogen, induction and acid-base components, respectively. Additionally, γ_s^o denotes all other interactions that may be present in the system.

Throughout any wettability study the effects of adsorption, evaporation and absorption of the measuring liquid on the solid surface should also be considered, especially during the research and development of inks and substrates for applications within the printing industry [28]. On account of this, numerous works have been conducted on adsorption [29,30], evaporation [28,31-34] and absorption [6,28,35,36] in relation to the wetting of materials. This highlights the importance of the liquid-material interface and environmental conditions (temperature, humidity and air pressure etc.) for inkjet-based applications. This is owed to the fact that the material properties, liquid properties and the environmental parameters will have a large influence on the adsorption, evaporation and absorption processes taking place.

When physically measuring the contact angle, θ, on a solid surface, many conventional techniques implement µl volume droplet sizes [37-40]. One of the most used techniques is that of the sessile drop method which uses a liquid drop placed with a syringe on the solid surface. The static contact angle is measured when the contact area is constant and in equilibrium [34,41,42]. Whilst this is a commonly utilised method, it does not always account for any variations in surface roughness as the µl droplet range is macroscopic in comparison to the solid surface features which make up the surface roughness [43]. This gives rise to the

measurement of an apparent contact angle, θ^{app}, rather than the actual contact angle. Furthermore, by taking specific ink jet printing technologies into account, the printing process tends to be within microscopic dimensions (which would require pl-range volumetric droplets). With µl-range droplets giving rise to apparent contact angles, θ^{app}, along with likely variations in absorption properties and evaporation properties for the different ranged droplet sizes [44,45], it is crucial to consider the droplet size during any wettability science study for ink/substrate applications. As a result, it could be argued that, for ink/substrate applications, pl-range droplet volumes should be utilised as this would be the same size as the structures/pores of the substrate (~100µm). It would also lead to $\theta^{app} \approx \theta$ and the pl-range would provide a similar volume as a typical printing process. Therefore, the pl-sized droplet would likely exhibit similar absorption and evaporation behaviours to that seen with the actual ink jet printing. This corresponds with droplet volume/contact angle studies which have been conducted for oil recovery mechanisms [46] and food contact surface properties [47]. This has also led to some previous fundamental studies on pl-sized droplet wettability studies [42,48]. Given the importance of droplet size to the ink/substrate industry, this work details the differences in contact angle measurement between µl-range droplets and pl-range droplets on commercially available coated and non-coated paper. That is the variation on contact angle measurement, absorption behaviour and evaporation behaviour are considered and discussed, highlighting the importance of using pl-range droplets in the development of ink and associated substrates.

Experimental Details

Materials

Standard, commercially available paper and printing inks were used throughout the experimentation. Specific details of the paper and printing inks are detailed below.

Paper and Silicon Wafer Substrates

Commercially available double-coated paper was used, with a grammage of 130g/m². In comparison a commercially available non-coated bleached paper with a grammage of 135g/m² was used for experimentation. All grammage was in accordance with standard ISO 536. The thickness of both paper samples was 125±5 µm and 135±5 µm for the coated and non-coated paper, respectively. To verify the specified thicknesses, a micro-screw was implemented on both samples. An average thickness was determined for each sample by repeating the measurements ten times over ten different locations on each of the samples.

A silicon wafer sample was implemented as a non-absorptive, flat and inert media to determine the drop volumes. 150 mm diameter silicon wafer was mechanically cut into smaller pieces, rinse with iso-propanol and air dried prior to any measurements taken.

Printing Inks

A commercially available water-based blue ink was used on the various substrates. The density of 1,0833g/cm³ was determined using a tensiometer (DCAT 25, DataPhysics Instruments GmbH, Germany). The surface tension was determined using the pendant drop method with a goniometer (OCA 200, DataPhysics Instruments GmbH, Germany). From using this method, the surface tension, SFT, was determined to be 65.8 mN/m (SFTd = 36.4 mN/m; SFTp = 29.4 mN/m). This was determined by interfacial tension (IFT) against n-Dodecane.

For verification purposes, commercially available water-based black ink was used on the substrates. Using both the tensiometer and goniometer both the density and surface tension of these two inks were determined. The black ink had a density of 1,1306 g/cm³ and an SFT of 36.8 mN/m (SFTd= 27.8 mN/m; SFTp=9.0 mN/m).

Wettability Measuring Liquids

Three liquids were used to conduct wettability characteristic measurements of the sample substrates. These were deionized water, diiodomethane and ethylene glycol. The deionized water had an SFT of 72.8 mN/m as per the Ström database in the SCA20 software which operated the goniometer. The diiodomethane (99%, ReagentPlus, Sigma-Aldrich, Germany), containing copper as a stabilizer had an SFT of 50.3 mM/m. The ethylene glycol puriss P.A. (>99.5% (GC), Honeywell Fluka, Germany) had an SFT of 48 mN/m.

All the SFT values were also experimentally verified by employing the goniometer (OCA 200, DataPhysics Instruments GmbH, Germany) to measure each of the liquids.

Wettability Analysis

Microlitre (µl) Wettability Analysis

µl wettability analysis was carried out using a goniometer (OCA 200; DataPhysics Instruments GmbH; Germany). The contact angles, θ, of water, diiodomethane, ethylene glycol and inks on the various paper substrates, detailed in Section 2.1, were determined using the quasi-static

contact angle measurement method, given that absorption and evaporation does occur over time. The surface energy was determined by applying the Owens, Wendt, Rabel and Kaeble (OWRK) [23] approach, as defined by Equation (3), to calculating surface energies. Each θ was determined by recording a movie with a high framerate and evaluating the θ (ellipse fitting) image by image and taking the contact angle at which point the base diameter did not increase. In all instances, the liquid droplet θ was evaluated at the moment when the base diameter/wetted area was deemed constant and wetting was complete whilst evaporation/absorption was still in occurrence.

Picolitre (pl) Wettability Analysis and Printing Emulation

pl wettability analysis was carried out using a goniometer (OCA200; DataPhysics Instruments GmbH; Germany) with a picolitre dosing system (PDDS; DataPhysics Instruments GmbH; Germany). Acoustic pulse generated droplets were placed on to the paper substrates with dosing volumes between 15 pl and 380 pl. The dispensing frequency used was between 100 Hz and 200 Hz. The amplitude and width of the dispensing pulse was individually optimized before every measurement with the integrated drop-watcher/strobe function to make sure only one stable drop, without satellites, was dispensed. For the incident liquid droplets, volumes between 50 pl and 100pl were used for θ measurements. Similar to the µl wettability analysis, θ was measured for the pl experimentation once the wetting was complete and there were no further changes in the droplet base diameter or wetted area.

The OCA200 along with PDDS was also implemented to emulate an industrial printing process following wettability analysis. This enabled verification of the wettability characteristic findings. To emulate the printing process, the dispensing pulse width and dispensing amplitude was optimized through experimentation before measurements were taken. The dispensing frequency was set constant at 20 Hz and the automated stage y-axis velocity was set constant at 2 mm/s resulting in 10 droplets/mm.

Environmental Conditions

To ensure consistency of results, all wettability measurements and experiments were conducted within a climate controlled laboratory with the temperature remaining constant at 22±0.5 °C and humidity was kept constant at 45±5%.

Absorption Analysis

For absorption analysis, either one drop of volume 48 pL or 20 drops of volume 910pL, with a dispensing frequency of 1000Hz, were dispensed on to the substrate. The liquid used for the absorption analysis was ethylene glycol puriss P.A. (>99.5% (GC), Honeywell Fluka, Germany). The camera framerate was constant at 1000 frames per second. A movie was recorded from the moment of dispensing and starting with the first image showing contact between ink and substrate the contact angle was calculated image by image. Since the software always calculated the volume, base diameter and many other values of interest along with the contact angle, and since the image was referenced in advance with the PDDS Reference Standard (100µm), the volume of the drop and contact angle could be plotted against time.

Results and Discussion

Wetting Behaviour at Different Dimensions

Figure 3 shows a graph of contact angle as a function of time for the water-based black ink on a paper substrate for conventional µl-sized droplets compared with pl-sized droplets. It can be seen from Figure 3 that the largest variation between the two dimensioned droplet systems occured within the first 20 ms whereby the pl volume droplets gave rise to a contact angle of 47.2±3° and the µl volume droplets gave rise to a contact angle of 32.1±1°, at time 0 s. This can be explained with two considerations. Firstly, conventional dispensing, as occurred with the µl droplet dosing system, did not allow for the immediate determination and measurement of the contact angle upon first initial contact between the liquid and the surface. This was because of the amount of time taken for the droplet to form an equilibrium state which can be measured. The second consideration is that the variations between the µl droplets and the pl droplets could have given rise to significant differences with regards to absorption, something of which is critical for inkjet applications. Another important result which can be taken from Figure 3 is that the initial contact angle is higher for the pl-sized droplets when compared to the µl-sized droplets. Then, after a few ms, the pl-sized droplets gave rise to contact angle values less than that observed with the µl-sized droplets. This was likely due to the differences in absorption characteristics for the two differently dimensioned droplets with the µl-sized droplet being impacted upon less due to absorption compared to the smaller pl-sized droplet. Extrapolating from the data shown in Figure 3, once the droplet was fully absorbed (with zero volume) the contact angles were determined to be 14.9° for the µl-sized black ink droplets and 14.7° for the pl-sized black ink droplets. The variations in contact angle observed between the pl-sized and µl-sized droplets, which are also evidenced in Figure 4 (water-based blue ink) and

Figure 5 (water) ($\theta_{pl} < \theta_{\mu l}$), highlights further the potential for tunable wetting surfaces when considering droplet size which has already been shown for µl-sized droplets [49,50].

The variations observed between the pl volume droplets and the µl volume droplets contradicts the work of Cansoy [51] who showed that droplet volume variation did not significantly impact on the contact angles measured, with the results showing that the contact angle was similar for all droplet volumes incident on micro-patterned surfaces coated with dimethyldichlorosilane (DMDCS). This is significant as it shows that there is likely a major different between studying non-absorptive materials, which was the case with Cansoy [51], and absorptive materials which is the case with this study. In order to further confirm this, the contact angle of deionized water at varied droplet volumes was studied on silicon wafer substrates (a non-absorptive material) as a comparison. Figure 6 shows a histogram of the contact angle for deionized water droplet volumes ranging between 40 pl and 2,200 pl, highlighting that the contact angle remained somewhat constant at around θ=70° over the large range of droplet volumes. Taking Figure 3, Figure 6 and the work of Cansoy [51] into account, it is highly likely that the second consideration has given rise to the difference in contact angle observed between the µl volume droplets and the pl volume droplets. That is, the difference in droplet volume gave rise to significant differences in absorption characteristics of the black ink, leading to variations in the measured contact angle between the two droplet volumes as evidenced in Figure 3.

To determine if the contact angle was influenced by drop size or dispensing method, the PDDS pl droplet dispensing system was implemented to place water-based ink on to absorbing paper substrates. The PDDS pl droplet dispensing system was used to place droplets of 3 different volumes; 500pl, 10 nl and 0.2 µl, as shown in Figure 4. As one can see from Figure 4, there was a variation of 35.5° between the 77.9° contact angle obtained with the 500 pl droplet and 113.4° with the 0.2 µl droplet. Because the three water-based blue ink droplets, shown in Figure 4, were dispensed via the PDDS droplet system, it stands to reason that the value of contact angle is dependent on the droplet size rather than the dispensing method. This is further verified with PDDS dispensed deionized water droplets on the absorbing paper as similar differences in the contact angles were observed (θ_{pl} = 68°, $\theta_{p\mu l}$ = 104° and $\theta_{\mu l}$ = 102°). This data shows that a pl droplet gave a θ (68°) around 36° less than that of the µl droplets which were dispensed by both the PDDS (θ = 104°) and the standard µl goniometer equipment (θ = 102°), both of which gave rise to θ of around 100°. Taking this data into account, the wetting behaviour of industrial

printing paper in terms of contact angle is determined by the droplet volume and is independent of the dispensing method used.

Figure 5 shows three shadowgraphs of water droplets with three different volumes (250 pl, 30 nl and 0.8 µl) in static equilibrium on the non-coated, slightly absorbing paper. Whilst the 250 pl water droplet gave rise to a lower contact angle of 38.7°, the 30 nl and 0.8 µl water droplets gave rise to similar contact angles of 57.5° and 55.9°, respectively. This is owed to the fact that the water droplet volumes were larger than the surface topography structure and the pore dimensions. As soon as the water droplet is of the same dimensions, or smaller, as the surface structure or pore dimensions this will have a large effect on the values of the contact angle. This shows that the droplet size in comparison to the parameters of the measured surface is very important when determining the contact angle. When studying the droplets of water on non-structured surfaces, like the silicon wafer (see Figure 6), the smallest pl droplets showed the same contact angle as nl droplets and µl droplets, again showing that the surface structure in comparison with drop sizes in the same range are the main reason for the differences in contact angle.

Absorption and Evaporation Behaviour

Figure 7 shows graphs of the contact angle and drop volume as a function of droplet age for both the coated and non-coated paper. In the initial instance ($t<0.04$ s) of the ethylene glycol droplet coming into contact with the two paper samples, it was observed that bigger droplet volumes absorbed slightly faster compared to when the droplet reduced in volume. This may suggest that the absorption may be promoted by gravitational force. After $t = 0.04$ s, the absorption process showed that the volume decreased linearly over time and one can therefore calculate the absorption rate as the slope of this decrease. Following a duration of approximately one to two seconds, the droplet was observed to be completely absorbed in both cases for the coated and non-coated paper. Figure 7(d) shows a graph of contact angle as a function of droplet volume for the ethylene glycol on both the coated and non-coated paper. Through the method of extrapolation from the linear relationship ($t>0.04$ s), as shown in Figure 7(d), it was found that the contact angles of the ethylene glycol on the coated and non-coated paper was 12.2° and 6.8°, respectively, as the volume tended towards zero.

There is evaporation to be considered and one cannot distinguish experimentally, in this instance, between absorption and evaporation. Having said that, it is commonly known that the

evaporation times of water and water-based inks are of the order of 10 s to 100 s [31-33,45,52] whereas absorption times take place in the region of less than a second. Because of this, it has been assumed that the evaporation time is negligible in this instance compared to that of absorption. One additional consideration to identify which process is taking place is the drop base diameter. During evaporation the diameter stays constant for a while due to the adhesion of the liquid on the surface. This is then followed by a retraction of the liquid front [37]. For absorption, on the other hand and as was observed during experimentation, the base diameter decreases (for $\theta<90°$) or first increases (for $\theta>90°$) and then decreases since the widest part of the drop is the one of the half sphere at 90°. It should also be noted that measurements were also performed on silicon wafer substrates (see Figure 4), a non-absorptive material, and the evaporation of the liquid droplets at the studied droplet volumes and dimensions was in the range of a few seconds to ten seconds, therefore it can be assumed that evaporation was negligible compared to the absorption which was observed to completely take place between one and two seconds.

Wettability Characterization and Wetting Behaviour Prediction

For many printing applications, it is known that coated paper substrates, with a flat, less rough surface contour is needed to produce sharp, well defined printed features. Taking this into consideration, some ink manufacturers have developed commercially available inks upon which it is claimed that newly developed inks do not need coated paper substrates to produce the desired printing quality. To determine if this is the case, commercially available non-coated paper, coated paper, water-based blue ink and water-based black ink was chosen, with the wettability parameters characterized through experimentation. Table 1 shows the contact angles, surface free energies and surface tension for the coated paper, non-coated paper and the two water-based inks.

From Table 1, the coated paper exhibited a higher surface free energy, with higher polar parts compared to that of the non-coated paper. Leading on from this, having characterised the wettability parameters for the two variations of paper, wetting envelopes could be drawn showing lines of contact angle/wetting behaviour with the two inks plotted (see Figure 8). From the wetting envelopes, shown in Figure 8, the predicted contact angles for the water-based blue and black inks were determined and are given in Table 2. This enabled a prediction to be made in that the commercially available water-based blue ink would not spread on either paper types, whereas spreading would likely occur with the water-based black ink. This is owed to the fact

that the contact angles for the water-based black ink was considerably smaller with predictions of 27° and 0° for the coated paper and non-coated paper, respectively.

To verify the prediction for water-based blue ink, following the development of the wetting envelope, 500 pl of the commercially available blue ink was dispensed using the PDDS pl droplet dispensing systems onto coated and non-coated paper substrates. Figure 9 shows that the commercially available blue ink gave rise to a contact angle of 34° on the coated paper substrates and 70° on the non-coated paper. Whilst the absolute values differ from the predicted values, the initial prediction of non-spreading was verified. That is, spreading did not occur on either of the paper substrates and the contact angle was higher on the non-coated substrate. It should also be noted that little to no absorption was observed for the water-based blue ink. In addition, with regards to printing applications, the results show that the water-based blue ink is capable of being used in printing applications to produce clear and sharp contours, without the need of coating the paper substrate.

Emulating the Printing Process

To verify the results from the PDDS wetting behaviour experimentation (see Section 3.3) the OCA200 was implemented to emulate the commercial printing process. Figure 10 shows the emulated printing process for the water-based blue ink on the non-coated paper (Figure 10(a)) and for the water-based black ink on the non-coated paper (Figure 10(b)).

From Figure 10(a), the water-based blue ink printed on to the non-coated paper gave rise to a clear contour, with no dissolving of the ink onto the paper. This verified that the ink was optimised for this particular non-coated paper, as predicted by the analysis of the wettability characteristics which was discussed in Section 3.3. Figure 10(b) shows the spreading and dissolving of the water-based black ink on the non-coated paper for comparison giving rise to a poorer and less sharp contour. This highlights how the pl volume range droplet sizes can be implemented to estimate how printing inks are going to perform with paper substrates. By employing such a wettability analysis process described within this work, it is highly likely that those in the ink/printing substrate will be able to enhance their research and development, becoming more efficient and effective as a result.

Conclusions

Through the study of a newly developed, commercially available water-based blue ink, a picolitre droplet dispensing system (PDDS) was implemented to determine the inks wettability characteristics on both coated and non-coated paper, predicting that the ink could be used to produce clear and sharp contours, compared to a another commercially available, water-based black ink. Furthermore, the PDDS was used to emulate an industrial printing process to verify that the newly developed blue ink did indeed produce clear and sharp contours on non-coated paper.

For many surface adhesion applications, wetting analysis is a powerful tool which can be used to enhance wettability and adhesion properties. This is especially the case for printing applications and the development of inks for printing as it ensures that effort and costs are minimized. Upon studying the differences between µl and pl droplet volumes, it has been shown that, for industrial inkjet printing applications, pl droplet volumes should be implemented during the study of the wettability characteristics. This is owed to the fact that the contact angle is very much dependant on droplet volume on structured/pore-consisting surfaces (absorptive and non-absorptive surfaces), and the droplet volume for experimentation should be carefully considered and chosen to align closely with the application under consideration. It has also been evidenced within this work that the contact angle is independent of the contact angle measuring method.

References

1. Paint, Coatings & Printing Ink Manufacturing - UK Market Research Report. IBISWorld Market Research Reports, October 2018.

2. I Printing Inks Market - Segmented by Type, Process, and Application - Growth, Trends, and Forecast (2019 - 2024**)**. Mordor Intelligence Industry Reports, October 2018.

3. Soltman, D., Smith, B., Kang, H., Morris, S.J.S., Subramanian, V., Methodology for inkjet printing of partially wetting films. Langmuir 2010 26, 15686-15693.

4. de Gans, B., Schubert, U.S,. Inkjet printing of well-defined polymer dots and arrays. *Langmuir* **2004** 20, 7789-7793.

5. Vaithilingam, J., Saleh, E,. Körner, L., Wildman, R.D., Hague, R.J.M., Leach, R.K., Tuck, C.J., 3-Dimensional inkjet printing of macro structures from silver nanoparticles. *Mater. Des.* **2018** 139, 81-88.

6. Öhlund, T., Örtegren, J., Forsberg, S., Nilsson, H., Paper surfaces for metal nanoparticle inkjet printing. *Appl. Surf. Sci.* **2012** 259, 731-739.

7. Lee, J., Kweon, J., Cho, W., Kim, J., Hwang, K., Hwang, H., Han, K.-S., Formulation and characterization of black ceramic ink for a digital ink-jet printing. *Ceram. Int.* **2018** 44, 14151-14157.

8. Soltman, D., Subramanian, V., Inkjet-printed line morphologies and temperature control of the coffee ring effect. *Langmuir* **2008** 24, 2224-2231.

9. Young, T., Hydraulic investigations, subservient to an intended Croonian lecture on the motion of the blood. *Philos. Trans. Royal Soc.* **1808** 98, 164-186.

10. Schrader, M.E., Young-Dupre revisited. *Langmuir* **1995** 11, 3585-3589.

11. Gould, R.F., Contact Angle, Wettability and Adhesion, Applied Publications, Washington D.C., USA, 1964.

12. Marmur, A., The lotus effect: Superhydrophobicity and metastability. *Langmuir* **2004** 20, 3517-3519.

13. Sung, Y.H., Kim, Y.D., Choi, H., Shin, R., Kang, S., Lee, H., Fabrication of superhydrophobic surfaces with nano-in-micro structures using UV-nanoimprint lithography and thermal shrinkage films. *Appl. Surf. Sci.* **2015** 349, 169-173.

14. Farshchian, B., Gatabi, J.R., Bernick, S.M., Park, S., Lee, G., Droopad, R., Kim, N., Laser-induced superhydrophobic grid patterns on PDMS for droplet arrays formation. *App. Surf. Sci.* **2017** 396, 359-365.

15. Law, K.Y., Highly wettable slippery surfaces: Self-cleaning effect and mechanism. *Int. J. Wettability Sci. Technol.* **2018** 1, 31-45.

16. Nayak, B.K., Caffrey, P.O., Speck, C.R., Gupta, M.C., Superhydrophobic surfaces by replication of micro/nano-structures fabricated by ultrafast-laser-microtexturing. *Appl. Surf. Sci.* **2013** 266, 27-32.

17. Zhang, M., Feng, S., Wang, L., Zheng, Y., Lotus effect in wetting and self-cleaning. *Biotribology* **2016** 5, 31-43.

18. Lawrence, J., Waugh, D.G., Creating superhydrophobic surface structures via the rose petal effect on stainless steel with a picosecond laser. *Lasers Eng.* **2018** 37, 125-134.

19. Ghosh, U.U., Nair, S., Das, A., Mukherjee, R., DasGupta, S., Replicating and resolving wetting and adhesion characteristics of a rose petal. *Colloids Surf. A: Physicochem. Eng. Aspects* **2019** 561, 9-17.

20. Ryu, S., Choo, S., Choi, H., Kim, C., Lee, H., Replication of rose petal surfaces using a nickel electroforming process and UV nanoimprint lithography. *Appl. Surf. Sci.* **2014** 322, 57-63.

21. Xiao, Y., Huang, W., Tsui, C.P., Wang, G., Tang, C.Y., Zhong, L., Ultrasonic atomization based fabrication of bio-inspired micro-nano-binary particles for superhydrophobic composite coatings with lotus/petal effect. *Composites B: Eng.* **2017** 121, 92-98.

22. Fowkes, F.M., Attractive forces at interfaces. *Ind. Eng. Chem. Res.* **1964** 56, 40-52.

23. Owens, D.K., Wendt, R.C., Estimation of the surface free energy of polymers. *J. Appl. Polym. Sci.* **1969** 13, 1741-1747.

24. Zenkiewicz, M., Methods for calculation of surface free energy of solids. *J. Achieve. Mater. Manufact. Eng.* **2007** 24, 137-145.

25. Waugh, D.G., Lawrence, J., Morgan, D.J., Thomas, C.L. Interaction of CO2 laser-modified nylon with osteoblast cells in relation to wettability. *Mater. Sci. Eng. C* **2009** 29, 2514-2524.

26. Waugh, D.G., Lawrence, J., Shukla, P., Modulating the wettability characteristics and bioactivity of polymeric materials using laser surface treatment. *J. Laser Appl.* **2016** 28, 022502.

27. Waugh, D.G., Lawrence, J., Wettability characteristics of laser surface engineered polymers. In: Mittal, K.L., Lei, W.S. (Eds.), Laser Technology: Applications in Adhesion and Related Areas, Scrivener Publishing LLC, New York, USA, 2018, pp. 99-122.

28. Wijshoff, H., Drop dynamics in the inkjet printing process. *Curr. Opin. Colloid Interface Sci* **2018** 36, 20-27.

29. Singh, G., Sharma, M., Vaish, R., Tunable surface adsorption and wettability of candle soot coated on ferroelectric ceramics. *J. Adv. Res.* **2019** 16, 35-42.

30. Li, J., Li, C., Yang, G., Li, C., Wettability transition on micro-nano hierarchical structured Ni20Cr coating surface by selective spontaneous adsorption during vacuum evacuation. *Mater. Chem. Phys.* **2018** 219, 292-302.

31. Erbil, H.Y., McHale, G., Newton, M.I., Drop evaporation on solid surfaces: Constant contact angle mode. *Langmuir* **2002** 18, 2636-2641.

32. Hu, H., Larson, R.G., Evaporation of a sessile droplet on a substrate. *J. Phys. Chem. B* **2002**, 106 1334-1344.

33. Semenov, S., Starov, V.M., Rubio, R.G., Agogo, H., Velarde, M.G., Evaporation of sessile water droplets: Universal behaviour in presence of contact angle hysteresis. *Colloids Surf. A: Physicochem. Eng. Aspects* **2011** 391, 135-144.

34. Song, H., Lee, Y., Jin, S., Kim, H., Yoo, J.Y., Prediction of sessile drop evaporation considering surface wettability. *Microelectron. Eng.* **2011** 88, 3249-3255.

35. Patrascioiu, A., Duocastella, M., Fernández-Pradas, J.M., Morenza, J.L., Serra, P., Liquids microprinting through a novel film-free femtosecond laser based technique. *Appl. Surf. Sci.* **2011** 257, 5190-5194.

36. Chen, Y., Jiang, B., Liu, L., Du, Y., Zhang, T., Zhao, L., Huang, Y.D., High ink absorption performance of inkjet printing based on SiO2@Al13 core-shell composites. *Appl. Surf. Sci.* **2018** 436, 995-1002.

37. Yuan, Y., Lee, T.R. Contact angle and wetting properties. In: G. Bracco, B. Holst (Eds.), Surface Science Techniques. Springer Series in Surface Sciences Volume 51, Springer, Berlin, Germany, 2013, pp. 3-34.

38. Bordács, S., Agod, A., Hórvölgyi, Z., Compression of Langmuir films composed of fine particles: Collapse mechanism and wettability. *Langmuir* **2006** 22, 6944-6950.

39. Öner, D., McCarthy, T.J., Ultrahydrophobic surfaces. Effects of topography length scales on wettability. *Langmuir* **2000** 16, 7777-7782.

40. Gardner, D.J., Generalla, N.C., Gunnells, D.W., Wolcott, M.P., Dynamic wettability of wood. *Langmuir* **1991** 7, 2498-2502.

41. Naikade, M., Fankhänel, B., Weber, L., Ortona, A., Stelter, M., Graule, T., Studying the wettability of Si and eutectic Si-Zr alloy on carbon and silicon carbide by sessile drop experiments. *J. Eur. Ceram. Soc.* **2019** 39, 735-742.

42. Drelich, J., Miller, J.D., Good, R.J., The Effect of Drop (Bubble) Size on Advancing and Receding Contact Angles for Heterogeneous and Rough Solid Surfaces as Observed with Sessile-Drop and Captive-Bubble Techniques. *J. Colloid Interf. Sci.* **1996** 179, 37-50.

43. Wang, R., Bai, S., Effect of droplet size on wetting behavior on laser textured SiC surface. *Appl. Surf. Sci.* **2015** 353, 564-567.

44. Molaeimanesh, G.R., Akbari, M.H., Role of wettability and water droplet size during water removal from a PEMFC GDL by lattice Boltzmann method. *Int. J. Hydrogen Energy* **2016** 41, 14872-14884.

45. Furuta, T., Sakai, M., Isobe, T., Nakajima, A., Evaporation behavior of microliter- and sub-nanoliter-scale water droplets on two different fluoroalkylsilane coatings. *Langmuir* **2009** 25, 11998-12001.

46. Shedid, S.A., Ghannam, M.T., Influences of droplet volume on contact angle of resevoir rocks. *Energy Sources* **2006** 27, 1085-1097.

47. McGuire, J., Yang, J., The effect of drop volum on contact angle. *J. Food Protect.* **1991** 54, 232-235.

48. Berson, A., Brown, P.S., Talbot, E.L., Badyal, J.P.S., Bain, C.D., Experimental investigation of the impact, spreading, and drying of picolitre droplets onto substrates with a broad range of wettabilities. NIP27, 27th International Conference on Digital Printing Technologies, Minneapolis, USA 2011; October 2-6.

49. Yao, X., Hu, Y., Grinthal, A., Wong, T-., Mahadevan, L., Aizenberg, J., Adaptive fluid-infused porous films with tunable transparency and wettability. *Nat. Mater.* **2013** 12, 529-534.

50. Cassie, A.B.D., Baxter S. Wettability of porous surfaces. *Trans. Faraday Soc.* **1944** 40, 546-551.

51. Cansoy, C.E., The effect of drop size on contact angle measurements of superhydrophobic surfaces. *Roy. Soc. Chem.* **2014** 4, 1197-1203.

52. Bormashenko, E., Musin, A., Zinigard, M., Evaporation of droplets on strongly and weakly pinning surfaces and dynamics of the triple line. *Colloids Surfs A: Physicochem. Eng. Aspects* **2011** 385, 235-240.

Table 1: Contact angles, surface free energies and surface tension for the coated paper, non-coated paper and the blue ink.

	$\theta_{diiodomethanc}$	$\theta_{ethylene\ glycol}$	θ_{water}
Non-coated paper	36°	48°	68°
Coated paper	42°	39°	38°
	σ_s (mN/m)	**$\sigma_s^{dispersive}$ (mN/m)**	**σ_s^{polar} (mN/m)**
Non-coated paper	40.5	30.0	20.5
Coated paper	53.1	18.7	34.4
	σ_l (mN/m)	**$\sigma_l^{dispersive}$ (mN/m)**	**σ_l^{polar} (mN/m)**
Water-based blue ink	65.8	36.4	29.4
Water-based black ink	36.8	27.8	9.0

Table 2: Predicted contact angles as determined by the wetting envelopes shown in Figure 5.

	Coated Paper	**Non-Coated Paper**
Predicted $\theta_{\text{blue ink}}$	41°	57°
Predicted $\theta_{\text{black ink}}$	27°	0°

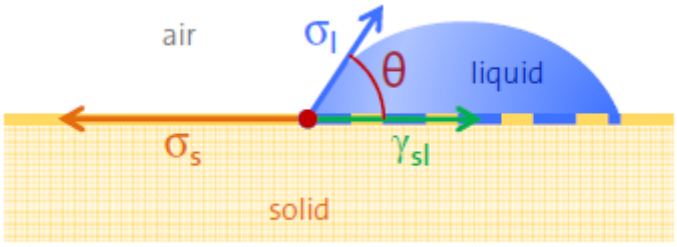

Figure 1: Schematic diagram showing a droplet of liquid on a solid surface, giving rise to the characteristic contact angle, θ.

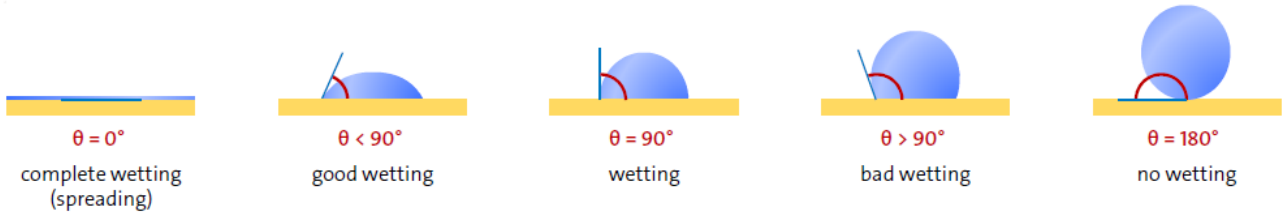

Figure 2: Schematic diagram showing the wetting nature at various values of contact angle.

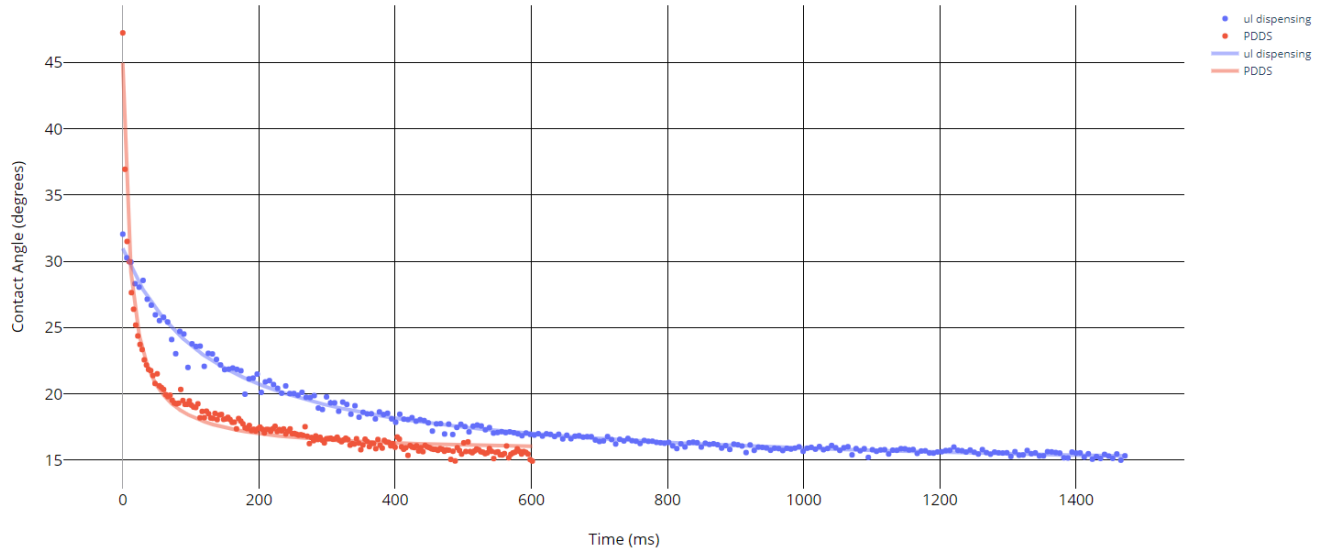

(a)

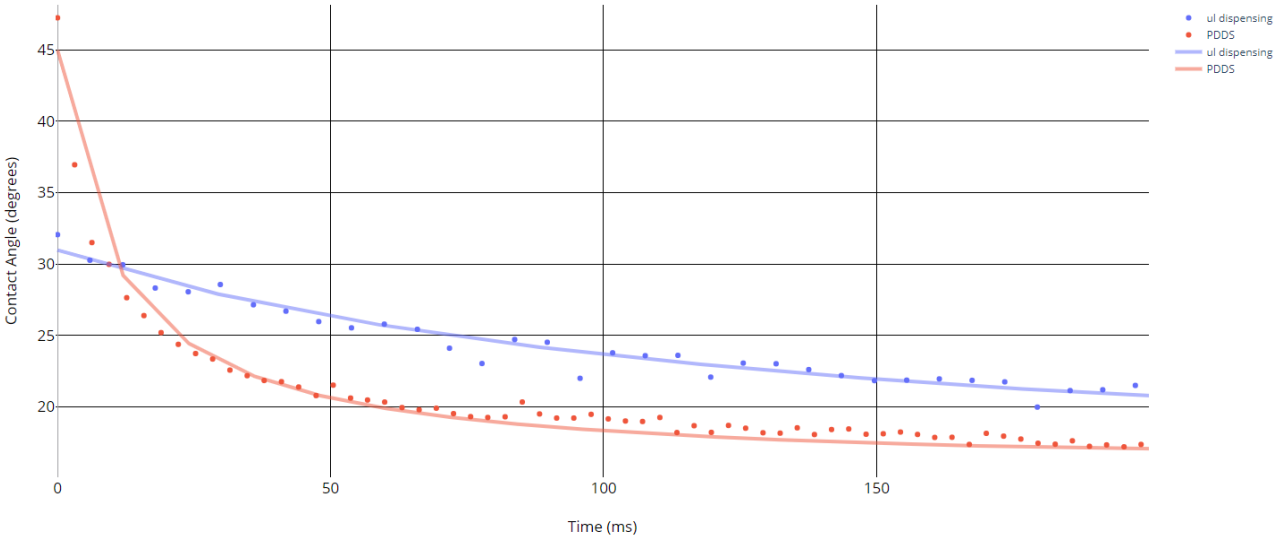

(b)

Figure 3: Graphs showing (a) the mean contact angle as a function of time for water-based black ink on the coated paper substrate and (b) the mean contact angle as a function of time for the first 200 ms for black ink on the coated paper substrate.

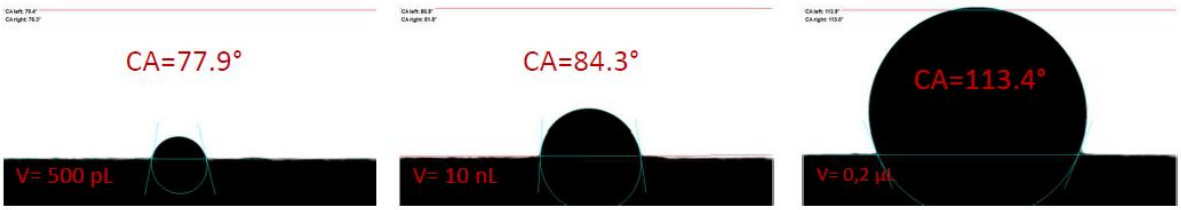

Figure 4: Shadowgraphs of PDDS pl dispensed droplets of water-based blue ink on an absorbing paper substrate for 3 different volumes: 500 pl, 10 nl and 0.2 µl.

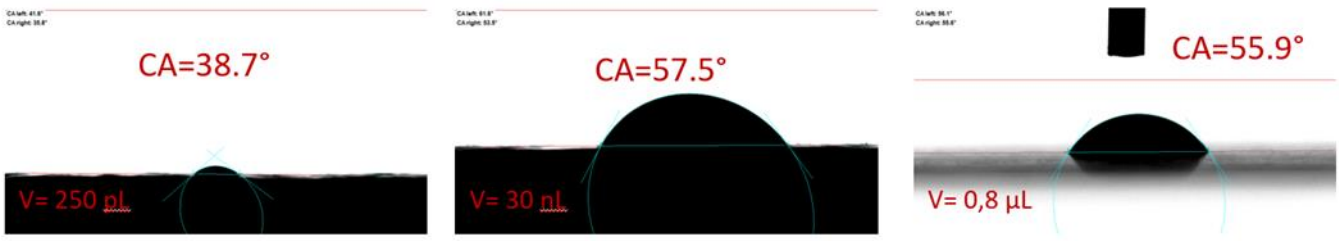

Figure 5: Shadowgraphs of three different water droplet volumes on the non-coated, slightly absorbing paper.

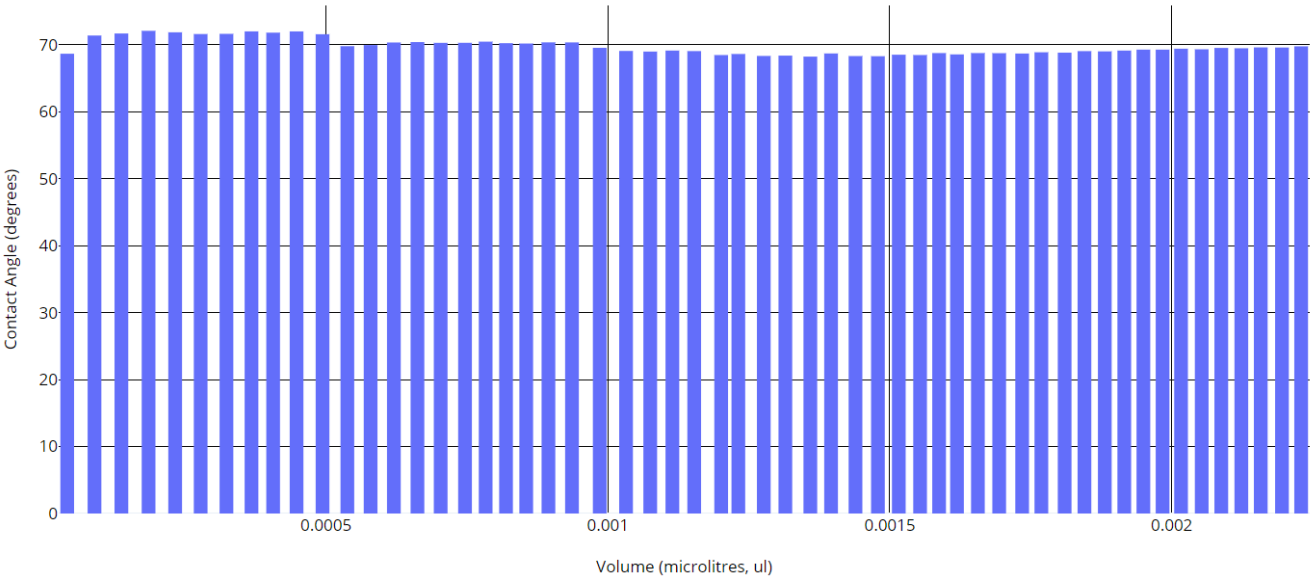

Figure 6: Histrogram showing the contact angle of water on a silicon wafer at droplet volumes between 40 pl and 2,200 pl.

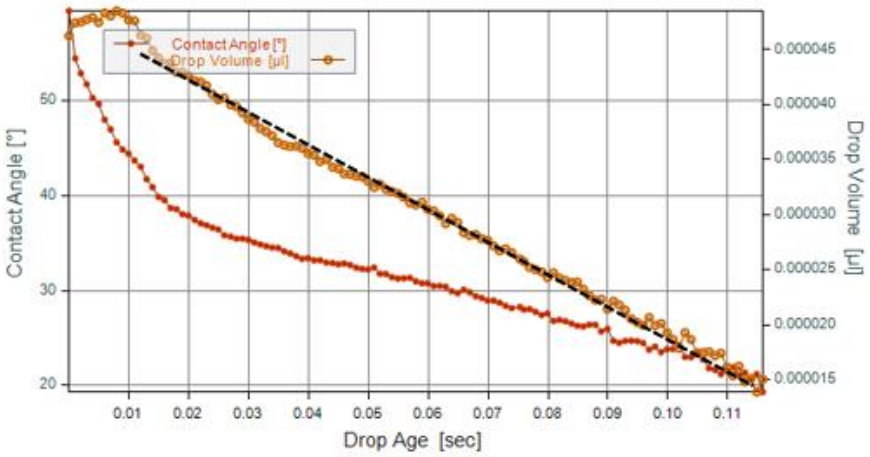

(a)

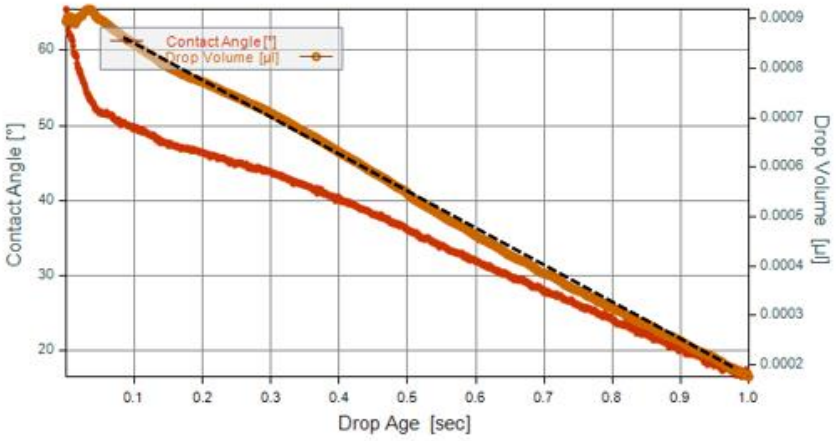

(b)

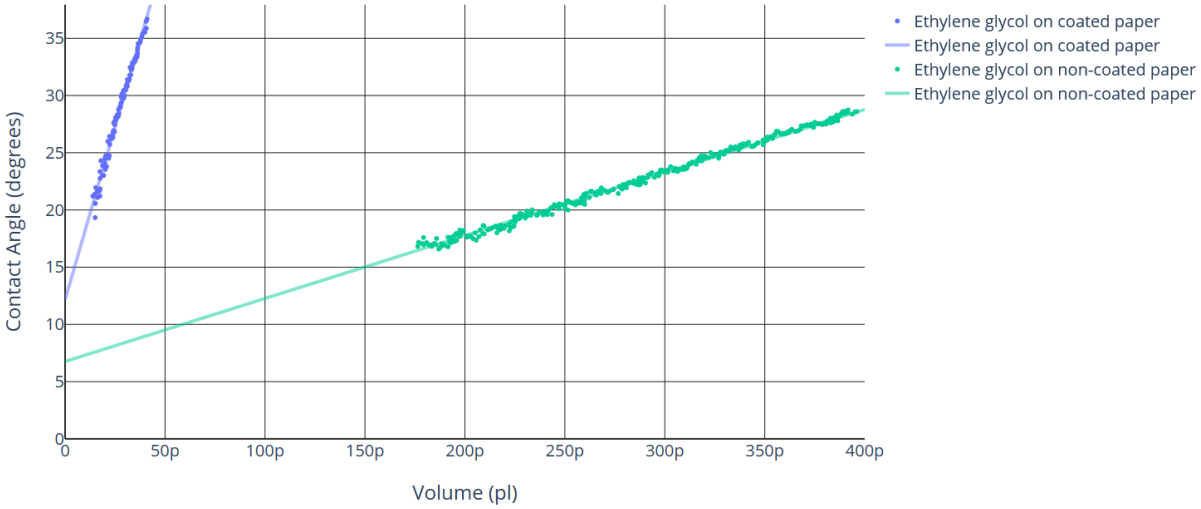

7(c)

Figure 7: Graphs showing (a) the contact angle and drop volume as a function of droplet age for ethylene glycol on the coated paper, (b) the contact angle and drop volume as a function

of droplet age for ethylene glycol on the non-coated paper and (c) the contact angle as a function of volume for the ethylene glycol on both the coated and non-coated paper.

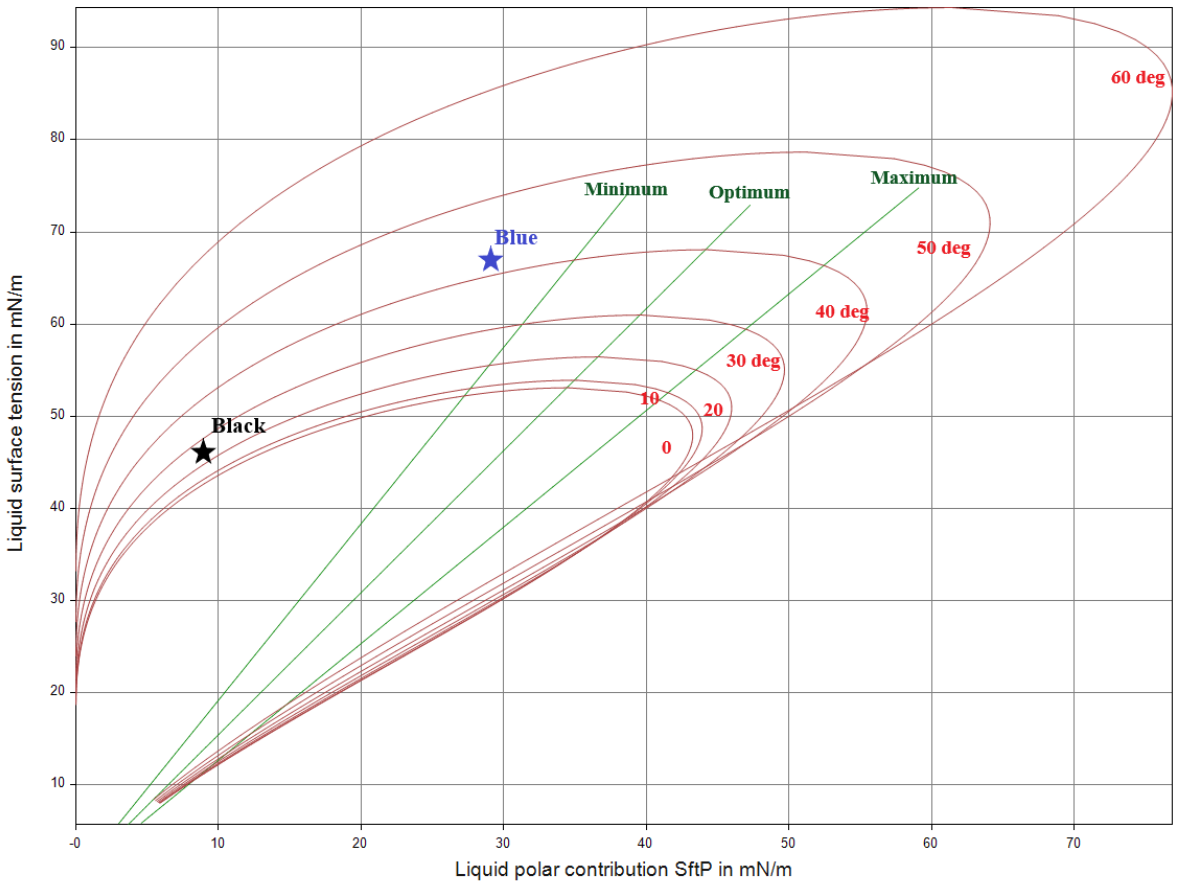
Liquid surface tension in mN/m
Liquid polar contribution SftP in mN/m
90
80
70
60
50
40
30
20
10
-0
10
20
30
40
50
60
70
Minimum
Optimum
Maximum
Blue
Black
60 deg
50 deg
40 deg
30 deg
20
10
0

(a)

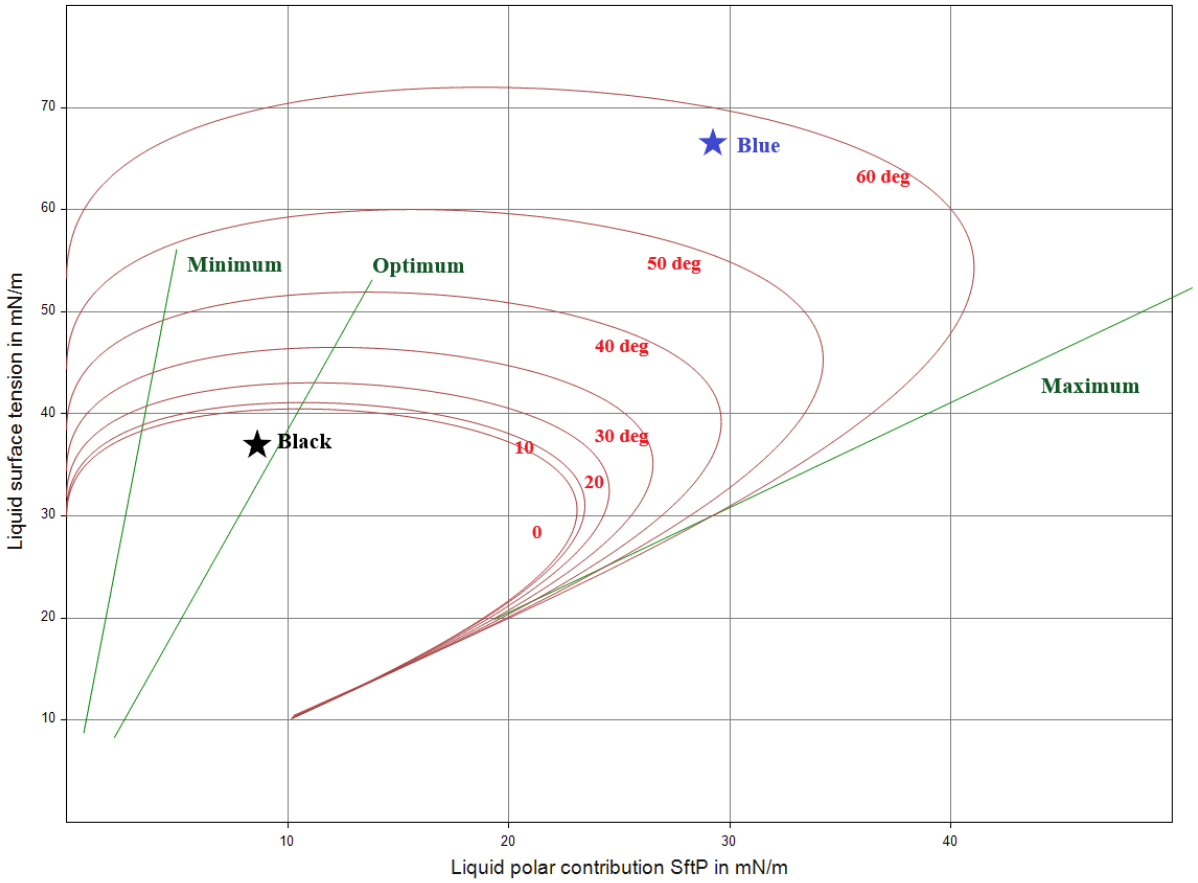

(b)

Figure 8: Wetting envelopes for contact angle/wetting behaviour for (a) the coated and (b) the non-coated paper. Red lines and text denote contact angle (°).

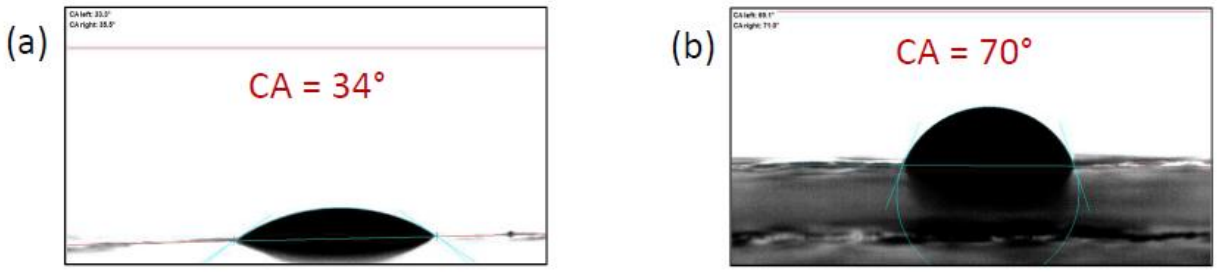

Figure 9: Shadowgraph images of the commercially available blue ink on the (a) coated paper and (b) non-coated substrates.

2.1.2

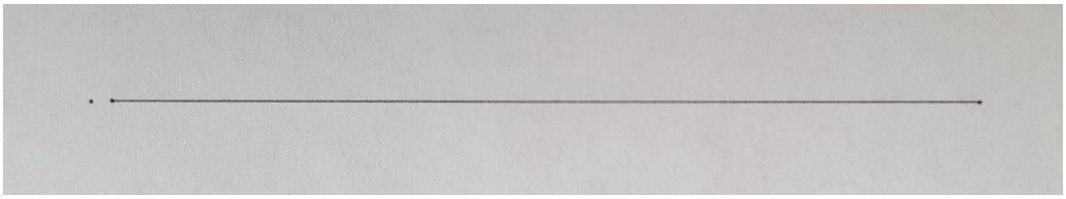

(a)

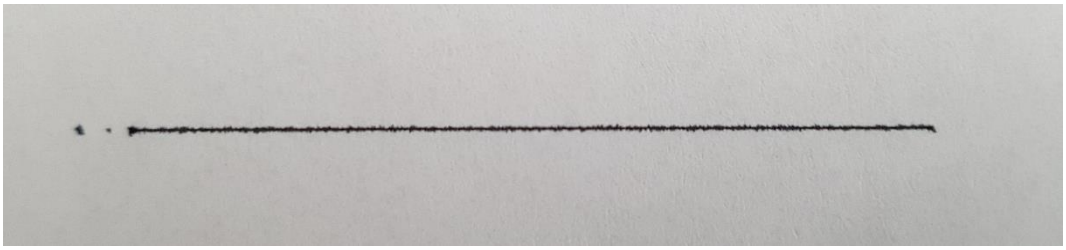

(b)

Figure 10: Images of the emulated printing process for (a) the blue ink on non-coated paper and (b) the black ink on non-coated paper.

For Table of Contents Use Only